Pressure dependence of dissociation fraction and optical emission characteristics in low-pressure inductively coupled N_2-Ar plasmas

T. H. Chung,[a] Y. W. Lee, H. M. Joh, and M. A. Song
Department of Physics, Dong-A University, Busan 604-714, Korea

(Received 8 April 2011; accepted 20 July 2011; published online 12 August 2011)

A diagnostics study of low-pressure inductively coupled N_2-Ar plasmas was performed by using optical emission spectroscopy (OES) and an rf-compensated Langmuir probe under the conditions of pressures of 1 - 30 mTorr and powers of 300 - 600 W. In the OES experiments, the argon was used as an actinometer and as an adding gas. The effect of the argon content in the gas mixture was examined in the range of 5 - 30%. The investigation of the effects of pressure on the dissociation fraction of nitrogen molecules and on the optical emission characteristics were carried out. The correction factors for estimating the dissociation fraction by OES actinometry accounting for argon effect were formulated and calculated. It was found that the dissociation fraction increased with increasing power and Ar content, while it decreased with increasing pressure. In addition, the electron energy probability function (EEPF), the electron density, and the electron temperature were obtained by using a Langmuir probe to investigate the effects of the plasma parameters on the optical emission characteristics and the dissociation fraction. [doi:10.1063/1.3628670]

I. INTRODUCTION

There has been a growing interest in the study of N_2 plasmas because of their potential use in the synthesis of nitride thin films and in the surface modification of various materials. Since atomic nitrogen plays an important role in the plasma processes, the determination of the absolute concentrations of N atoms in N_2 molecular discharges is crucial for understanding plasma process at the surface.[1–3] Electric discharges produced either by microwaves, helicon waves or radio frequency (rf) power are commonly used for generating nitrogen atoms.[2,4–6] Recently, there has been a steadily growing interest in the application of inductively coupled plasma (ICP) sources for numerous plasma-enhanced materials processing. It has been known that most of these plasma systems are characterized by high nitrogen atom content.[7]

The dissociation fraction in an inductively coupled nitrogen plasma is important for understanding and improving the nitridation processes because the number density of N atoms is deducible from the dissociation fraction. Generally, it is difficult to achieve a high dissociation efficiency of N_2 due to its extremely high bonding energy.[8] The dissociation of N_2 molecules in nitrogen plasmas has been diagnosed by using several techniques, such as mass spectrometry[9,10] and optical emission spectroscopy.[6,11,12] Nakano *et al.* measured the dissociation degree of N_2 in an inductively coupled plasma by using vacuum ultraviolet emission spectroscopy.[13] They observed that the dissociation fraction increased with the rf power when the N_2 pressure was kept at 4.98 mTorr.[13] In contrast, no large increase in the degree of N_2 dissociation with pressure was observed for a fixed rf power (1 kW) condition even when electron density increased sharply in the pressure range of 0.09 - 4.98 mTorr.[13]

[a]Email address: thchung@dau.ac.kr

Czerwiec *et al.* measured the dissociation fraction for an ICP sustained in a long cylindrical tube with a small radius specially designed for radical beam generation. They obtained a dissociation fraction from 0.1 (evaluated by using optical emission actinometry) up to 0.7 (by using mass spectrometry) for N_2 discharges at 50 mTorr.[9] In other articles, the degree of dissociation was found to be 1 - 4.9 %,[13] 0.58 - 4.4%,[8] 1 - 7%,[2] and 1% or below.[3,5,6] One of the promising ways to enhance the dissociation of molecular nitrogen is to introduce another gas such as hydrogen and argon in the plasma.[2] Tabbal *et al.* evaluated the nitrogen molecular dissociation level in N_2-Ar surface-wave plasma and observed the dissociation enhancement factor of 4.1 - 8.5 with the introduction of Ar to pure nitrogen discharges at the power of 60 - 120 W and the pressure of 7.6 Torr.[4]

In this study, N_2-Ar plasmas are produced with ICP sources. The production and loss mechanisms of N atoms in N_2-Ar discharges are very complex due to a huge set of reactions between charges species and neutrals (atomic and molecular nitrogen and argon atoms) including the wall interactions.[14,15] In our previous work,[16] we have shown that increasing the Ar content causes significant changes in the properties of discharge such as gas temperature, rovibrational excitation, electron energy distribution function, and dissociation fraction of N_2 molecules. A higher Ar content caused an enhancement of the dissociation fraction. It was found out that the calculated density of nitrogen atom was maximum at the Ar content of 30%.[16] A simple actinometry for N_2-Ar discharges with larger portion of Ar would give an overestimated value for dissociation fraction because the Penning excitation and/or dissociative excitation of nitrogen molecules due to all the excited states of Ar is usually neglected. In this work, we will determine the dissociation fraction more accurately by estimating the contributions from Ar excited states in more detail.

Another emphasis is placed on the effect of pressure on the dissociation fraction and discharge characteristics. For that purpose, the Ar content in the gas mixture is kept constant at 5% otherwise mentioned. This amount of Ar content allows us to apply the optical emission actinometry. But, as the pressure increases the amount of Ar gets larger, thus the interactions of the Ar atoms with neutrals and ions of atomic and molecular nitrogen become important. Especially, argon metastable atoms play an important role in the discharge kinetics, thereby influencing the dissociation of nitrogen molecules as well as rovibrational temperature. In this study, the density of argon metastables is calculated using a simple kinetics. This quantity is used to make a correction for determining the dissociation fraction by the optical emission actinometry.

The total pressure is varied in an attempt to fully characterize the optical emission characteristics of inductively coupled N_2-Ar discharges. We obtain the dissociation fraction by using optical emission actinometry at various powers (300 - 600 W) in the pressure range 1 - 30 mTorr, which is different from the range of similar studies.[3,4,8,13] A physical explanation of the variations of the dissociation fraction with pressure is given with a discussion of the particle balance and of plasma properties, such as the electron density, the electron temperature, and the electron energy probability function measured by using a rf-compensated Langmuir probe.

II. EXPERIMENT

A schematic diagram of the experimental setup with the diagnostics system (optical emission spectroscopy (OES), and rf-compensated Langmuir probe) is shown in Fig. 1. The plasma chamber consists of a stainless-steel cylinder with a 28-cm diameter and a 34-cm length. A 1.9-cm-thick by 27-cm-diameter tempered glass plate mounted on one end separates the planar one-turn induction coil from the plasma. The induction coil is made of copper (with water-cooling) and is connected to an L-type capacitive matching network and a rf power generator.

The plasma chamber is evacuated by using a diffusion pump backed by rotary pump giving a base pressure of 5×10^{-6} Torr. The equilibrium gas pressure in the chamber is monitored with a combination vacuum gauge (IMG 300). The operating gas pressure is controlled by adjusting the mass flow controller. The nitrogen gas pressure is varied in the range of 1 - 30 mTorr, and a 13.56 MHz generator (ENI OEM 12) drives an rf current in a flat one-turn coil through the rf power generator and matching network. The source gas is N_2 gas. We introduce Ar as an actinometer and as an adding gas for all cases.

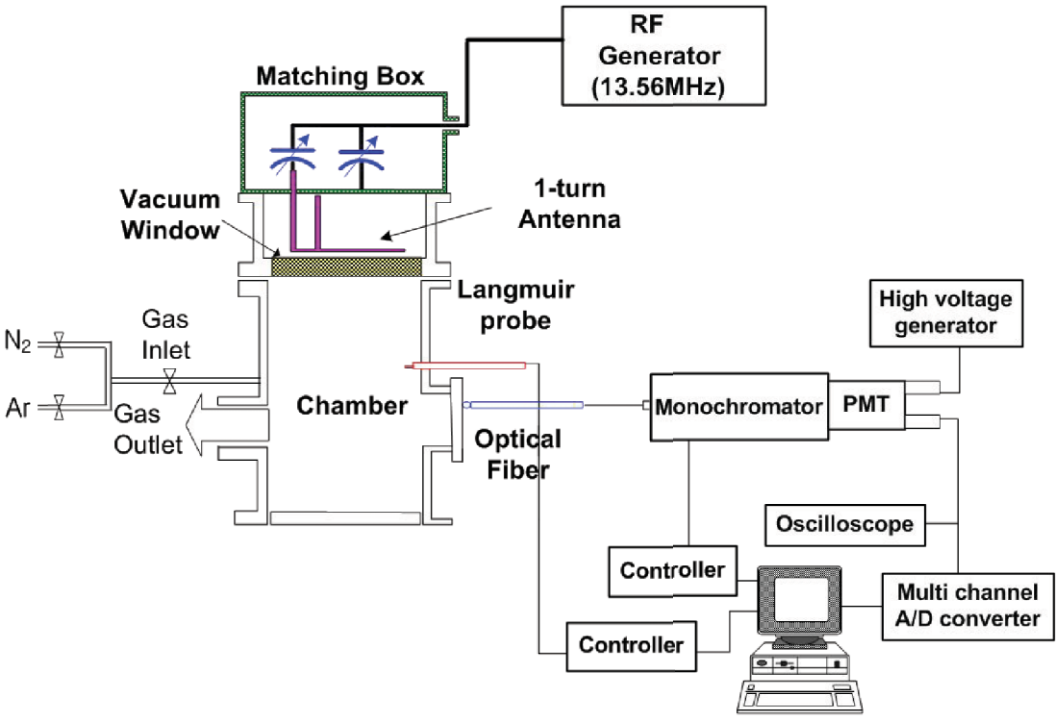

FIG. 1. (Color online) Schematic diagram of experimental set-up and diagnostics system.

An rf-compensated cylindrical single Langmuir probe was mounted through one of the ports on the vacuum chamber. The probe tip was located on the axis of the cylinder at 14 cm below the tempered glass plate. To measure the plasma parameters, the harmonic technique, which exploits the generation of harmonics resulting from excitation of the nonlinearity of the single Langmuir probe characteristics, combined with Druyvesteyn method was used. In the harmonic method, the voltage applied to the probe consists of the sweep voltage and the sinusoidal voltage v_0 of the frequency ω. Two signal generators were used to make 10 kHz of a small sinusoidal wave ($v_0 = 1.0$ V) and 1 Hz of a sawtooth wave. After being amplified by operational amplifiers, the sinusoidal signal was superimposed on the sawtooth signal swept from −30 V to 30 V. The superimposed signal was amplified by a power amplifier, and then applied to the probe tip though a resonance filter for 13.56 and 27.12 MHz to remove the rf fluctuation from the plasma potential. A cylindrical probe tip made of tungsten which is 0.1 mm in diameter and 10 mm in length was used. The current was obtained by measuring the voltage difference across the sensing resistor (100 Ω) using the differential amplifier. After data processing in the analog-to-digital converter, the fast Fourier transform was performed to find the second harmonic of the I-V characteristic. The second harmonic term $I_{2\omega}$ of the measured probe current is proportional to the second derivative as $I_{2\omega} \approx (1/4)\, v_0^2\, d^2I/dV^2 \cos 2\omega t$, which is related to the electron energy distribution function(EEDF), $f(\epsilon)$,

$$f(\epsilon) = \frac{2m}{e^2 S}\left(\frac{2eV}{m}\right)^{1/2} \frac{d^2I}{dV^2}, \tag{1}$$

where e is the electron charge, S is the probe area, m is the mass of electron, V is the probe potential referenced to the plasma potential (V_p), and ϵ is measured in units of eV. The electron density (n_e) and the effective electron temperature (T_e) are calculated with the measured EEDF as follows:

$$n_e = \int_0^{\epsilon_{max}} f(\epsilon)d\epsilon, \qquad T_e = \frac{2}{3n_e}\int_0^{\epsilon_{max}} \epsilon f(\epsilon)d\epsilon, \tag{2}$$

where ϵ_{max} is determined by the dynamic range of the EEDF measurement. The electron temperature can also be determined from the slope of the probe I-V curve in the exponential region (from the point

where the probe current is zero to where the slope of the curve begins to decrease). We observed that both methods yield almost same values of the electron temperature. The EEDF integral method has been used to obtain plasma parameters for many processing plasmas utilizing molecular gases.[17–20]

The light intensity of emissive molecules and radicals in the plasma was focused by means of optical fiber into entrance slit of 0.75 m monochromator (SPEX 1702), equipped with a grating of 1200 grooves per millimeter and slit width of 100 μm. The light was collimated at the exit slit where a photomultiplier tube (Hamamatsu R928) converted photons into an electric signal. Optical emission spectra were recorded in the wavelength range of 250 - 850 nm with a resolution of 0.1 nm. The measured emission spectra should be corrected for the spectral response of the detection system which includes optical fiber, monochromator, and photomultiplier tube. The detection system had to be calibrated in intensity between 250 to 850 nm using a quartz halogen lamp with a known spectral radiance.The dependence of the emission intensities on the plasma parameters is investigated. In plasma processing, actinometry is a frequently-used and well-developed technique to estimate the density of neutrals. In this method, a known concentration of an impurity is introduced, and the intensities of two neighboring spectral lines, one from the known gas and one from the sample, are compared. Since both species are bombarded by the same electron distribution and the concentration of the actinometer is known, the density of the sample can be calculated.

A kinetic analysis of a nitrogen discharge under the assumption of quasi-static equilibrium gives

$$[\mathrm{N}^*] = \frac{n_e[\mathrm{N}]k_N^{dir} + n_e[\mathrm{N}^m]k_{N^m}^{exc} + n_e[\mathrm{N}_2]k_{N_2}^{diss-exc} + [\mathrm{Ar}^m][\mathrm{N}]k_N^{Penn} + [\mathrm{Ar}^*][\mathrm{N}_2]k_N^{Penn-diss}}{\frac{1}{\tau_N} + k_{N^*}^{Q}[\mathrm{Ar}]}, \tag{3}$$

where n_e is the electron density, [N], [N*], and [N^m] are the population densities of the ground state, the excited state, and of the metastable state form of species N, respectively. And k_N^{dir} is the rate coefficient for electronic excitation of the ground state, $k_{N^m}^{exc}$ is the rate coefficient for electronic excitation of the metastable state, $k_{N_2}^{diss-exc}$ is the rate coefficient for electronic excitation through dissociation of molecule N_2, k_N^{Penn} is the rate coefficient for Penning excitation of the ground state N due to the excited states of Ar, $k_N^{Penn-diss}$ is the rate coefficient for Penning dissociation of N_2 due to the excited states of Ar, τ_N is the lifetime of the excited state and $k_{N^*}^{Q}$ is the rate coefficient for quenching by argon. Usually, at low-pressure discharges, $k_{N^*}^{Q}$[Ar] is much less than $1/\tau_N$ thus the quenching term can be neglected. The Ar metastables, $1s_5$ and $1s_3$, are at energy levels of 11.55 and 11.72 eV, respectively.[3] These metastables have significant interactions with nitrogen molecules through resonant energy transfer called Penning excitation and dissociation.

The emission intensity due to a transition from an excited level to a lower state is

$$I(\mathrm{N}^*) = K_N h\nu_N A_N[\mathrm{N}^*], \tag{4}$$

where K_N is a factor depending on plasma volume, solid angle and spectral response of the spectrometer, h is the Planck's constant, ν_N is the frequency of the transition, and A_N is the optical emission probability for the transition. and $k_{N^*}^{Q}$ are ignored, equation (4) can be expressed as

$$I(\mathrm{N}^*) = K_N h\nu_N A_N \tau_N n_e[\mathrm{N}]k_N^{dir}(1 + c_1). \tag{5}$$

where c_1 is the correction factor accounting for various contributions to the formation of excited nitrogen atoms rather than the direct excitation by electron impact. From equations (3) and (5), we have

$$c_1 = \frac{n_e[\mathrm{N}^m]k_{N^m}^{exc} + n_e[\mathrm{N}_2]k_{N_2}^{diss-exc} + [\mathrm{Ar}^m][\mathrm{N}]k_N^{Penn} + [\mathrm{Ar}^m][\mathrm{N}_2]k_N^{Penn-diss}}{n_e[\mathrm{N}]k_N^{dir}}. \tag{6}$$

The rate coefficients $k_{N^m}^{exc}$, $k_{N_2}^{diss-exc}$, k_N^{Penn}, $k_N^{Penn-diss}$ are less than k_N^{dir} by one order of magnitude. Unless the densities of metastable N and Ar atoms are large, the factor c_1 is small.

Similarly, the emission intensity from excited Ar atom is written as

$$I(\mathrm{Ar}^*) = K_{Ar} h\nu_{Ar} A_{Ar} \tau_{Ar} n_e[\mathrm{Ar}]k_{Ar}^{dir}(1 + c_2), \tag{7}$$

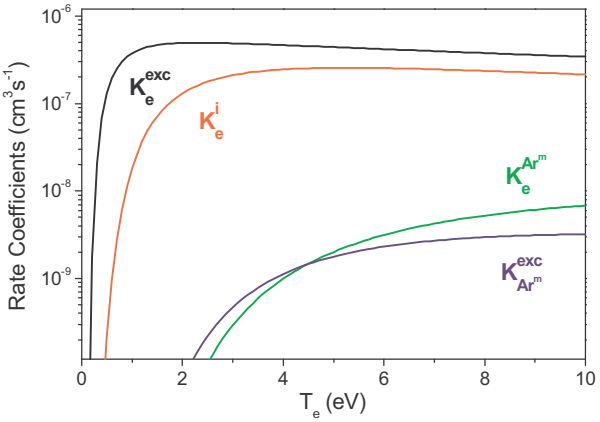

FIG. 2. (Color online) Rate coefficients for the direct excitation from the ground state to $1s_5$ ($k_e^{Ar^m}$), the direct excitation from $1s_3$ to $2p_1$ state ($k_{Ar^m}^{exc}$), and for the total excitation (k_e^{exc}) and ionization (k_e^i) from Ar metastable as a function of T_e.

where c_2 is the correction factor accounting for the excitation from the metastable Ar,

$$c_2 = \frac{[\mathrm{Ar^m}]k_{Ar^m}^{exc}}{[\mathrm{Ar}]k_{Ar}^{dir}}, \tag{8}$$

where $k_{Ar^m}^{exc}$ is the rate coefficient for the excitation of $\mathrm{Ar^m}(1s_3)$ to a specific higher ($2p_1$) state.

Density of metastable atoms is determined from the balance of the production (mainly by electron-impact excitation from the ground state ($k_e^{Ar^m}$)) and various loss mechanisms (excitation and ionization from metastable state, quenching, and diffusion induced wall loss).[21] A balance equation under the assumption of a quasi-static equilibrium gives

$$[\mathrm{Ar^m}] = \frac{k_e^{Ar^m} n_e [\mathrm{Ar}]}{(k_e^{exc} + k_e^Q + k_e^i)n_e + k_{N_2}^Q [\mathrm{N_2}] + k_{diff}}, \tag{9}$$

where k_e^{exc}, k_e^i, and k_e^Q are the rate coefficients for excitation and ionization from metastable state, and for electron-quenching of metastables, respectively. Here $k_{N_2}^Q$ is the quenching rate coefficient of $\mathrm{Ar^m}$ in N_2, and k_{diff} is the rate coefficient for diffusion induced wall losses expressed by $k_{diff} = D_{Ar}/(\Lambda^2$ [Ar]) where D_{Ar} is the diffusion constant of $\mathrm{Ar^m}$ in Ar ($D_{Ar} = 1.8 \times 10^{18} cm^{-1}s^{-1}$ is used) and Λ is the effective diffusion length of a cylinder of radius R and length L ($1/\Lambda^2 = (\pi/L)^2 + (2.405/R)^2$). The rate coefficients are calculated using the cross section data as

$$k_e^j = \sqrt{\frac{2e}{m}} \int_0^{\epsilon_{max}} \sigma_j(\epsilon)\sqrt{\epsilon} f(\epsilon) d\epsilon, \tag{10}$$

where σ_j is the electron-impact cross section of the collision type j. Utilizing the cross section data in the literature,[22–25] the rate coefficients for the direct excitation of the ground state Ar to $1s_5$ ($k_e^{Ar^m}$), the direct excitation of Ar metastables to $2p_1$ state ($k_{Ar^m}^{exc}$), and the total direct excitation and ionization of Ar metastables (k_e^{exc} and k_e^i) are computed and presented as a function of T_e in Fig. 2. In the operating region of this study, the values of $k_{N_2}^Q$ and k_e^Q are $3.6 \times 10^{-11}\mathrm{cm^3/s}$,[26] and $4 - 7 \times 10^{-8}\mathrm{cm^3/s}$, respectively.[24]

For the optical emission actinometry for N_2-Ar plasmas, the emissions of the N line at 746.68 nm ($3p\ ^4S_{3/2} \rightarrow 3s\ ^4P_{5/2}$) and the Ar line at 750.4 nm ($2p_1 \rightarrow 1s_2$ transition) are selected because they are not sensitive to two step excitation.

From equations (5) and (7),

$$\frac{[\mathrm{N}]}{[\mathrm{Ar}]} = \frac{I_{746}}{I_{750}} \frac{(1+c_2)}{(1+c_1)} \frac{K_{750}}{K_{746}} \frac{\nu_{750}}{\nu_{746}} \frac{A_{750}}{A_{746}} \frac{k_{Ar}^{dir}}{k_N^{dir}} \frac{\tau_{750}}{\tau_{746}}. \tag{11}$$

Then the dissociation fraction is derived as by[9,11]

$$\frac{[\mathrm{N}]}{[\mathrm{N_2}]} = 1.61 \frac{I_{746}}{I_{750}} \frac{(1+c_2)}{(1+c_1)} \frac{k_{Ar}^{dir}}{k_N^{dir}} \frac{x_{Ar}}{x_{N_2}}, \tag{12}$$

where x_{Ar} and x_{N_2} are the percentages of argon and nitrogen in the gas mixture with the discharge off. However, quantitatively accurate results can only be obtained if excitations via dissociative channels, Penning effect, and the quenching of excited states are accounted for.

In this experiment, using OES, we obtain the dissociation fraction for an inductively coupled N_2-Ar discharge as functions of Ar content, pressure, and applied ICP power. In order to better understand the effects of these parameters on the dissociation fraction, we measured EEPF (electron energy probability function), and the electron density, and the electron temperature by using a Langmuir probe.

III. RESULTS AND DISCUSSION

Figure 3 presents a typical optical emission spectrum of an ICP N_2-Ar plasmas operated in 1.4 mTorr at ICP power 500 W. The main emission peaks correspond to several transition lines of atomic nitrogen and argon and of molecular nitrogen. The spectrum is characterized by N_2 first positive band system (FPS)($B^3\Pi_g(v') \rightarrow A^3\Sigma_u^+(v'')$) and N_2 second positive band system (SPS)($C^3\Pi_u(v') \rightarrow B^3\Pi_g(v'')$), and N_2^+ first negative band system (FNS)($B^2\Sigma_u^+(v') \rightarrow X^2\Sigma_g^+(v'')$). Here v' and v'' are the vibrational quantum numbers of the upper and lower states and the vibrational transition is denoted simply as (v', v''). The spectra are dominated by strong molecular features, which peak around 300 - 400 nm and 600 - 800 nm. The total intensities of emission, from state $C^3\Pi_u$, and from state $B^3\Pi_g$, are changed as the pressure and ICP power vary. The emission intensities of all peaks significantly increased with power, while they overall decreased with pressure. The most intense emission intensities from N_2 second positive system are caused by many excitation and quenching processes such as the electron impact excitation from the ground state, the excitation from the first metastable state $N_2(A^3\Sigma_u^+)$ due to collision with metastable state Ar^m, which indicate the overpopulation of $N_2(C^3\Pi_u)$.[13,27] Therefore, it is observed that the most intense peak of the second positive system is large compared with the most intense peak of N_2 first positive system and N_2^+ first negative system. The reason for this phenomenon is the energy pooling reaction caused by effective lifetime of the first metastable state $N_2(A^3\Sigma_u^+)$ which has the lowest threshold energy (6.2 eV) and a long lifetime (about 2 s).[28] The Ar content in the gas mixture does not make a noticeable influence on the emission intensities of the typical lines of N_2 first and second positive systems and N_2^+ first negative system. By decreasing the amount of molecular N_2 with increasing the Ar content, excited atomic N and N_2^+ would also decrease. However, with the addition of Ar, Penning excitation and Penning dissociation due to Ar^m increase the densities of the excited states of N, N_2, and N_2^+ trading off the decrease in the amount of N_2. An increase in the Ar content results in a slight increase of the emission intensity from N atoms.

Figure 4 shows the emission spectra with the wavelength range of $250 - 450$ nm from N_2-5%Ar plasmas at different pressures. Many SPS bands ($\triangle v = -2, -1, 0, +1, +2, +3, +4$) and FNS bands ($\triangle v = 0, +1$) are clearly observed. Although not shown in the figure, the intensities from SPS at 5 mTorr increased compared to those at 1.4 mTorr. But, as the pressure further increases, the emission intensities of these bands decrease. The relative intensity of each bands vary depending on the pressure. For instance, in the plasma at 11 mTorr, the relative intensity from the SPS $\triangle v = +2$ transition is larger than that from the SPS $\triangle v = +1$ transition. With increasing pressure, the emission intensities of FNS (0,0) at 391.4 nm exhibits a significant change. The intensity ratio of $I_{391.4}$ to $I_{337.1}$ (SPS (0,0)) is decreased drastically at 11 mTorr, but rises at 22 mTorr and then decreases again at 30 mTorr. This complicated variations result from the changes of n_e, T_e, and neutral particle densities with pressure. Also the intensity from the SPS $\triangle v = +2$ sequence follows a similar change to those of FNS at 391.4 nm. These can be explained by the effects of N_2 supply and a subsequent decrease in T_e with pressure. These two effects act oppositely. As pressure increases, T_e decreases, thus the electron-impact vibrational excitation to higher levels are reduced. However, the number density of N_2 molecules is increased with pressure, thus the event of vibrational excitation (and

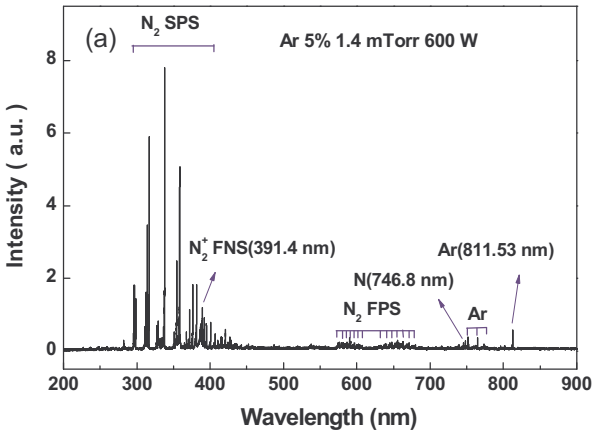

FIG. 3. (Color online) Spectrum of optical emission from inductively coupled N_2-Ar discharge at $p = 1.4$ mTorr and $P = 600$ W. Feed gas compositions are 5% Ar and 95 % N_2.

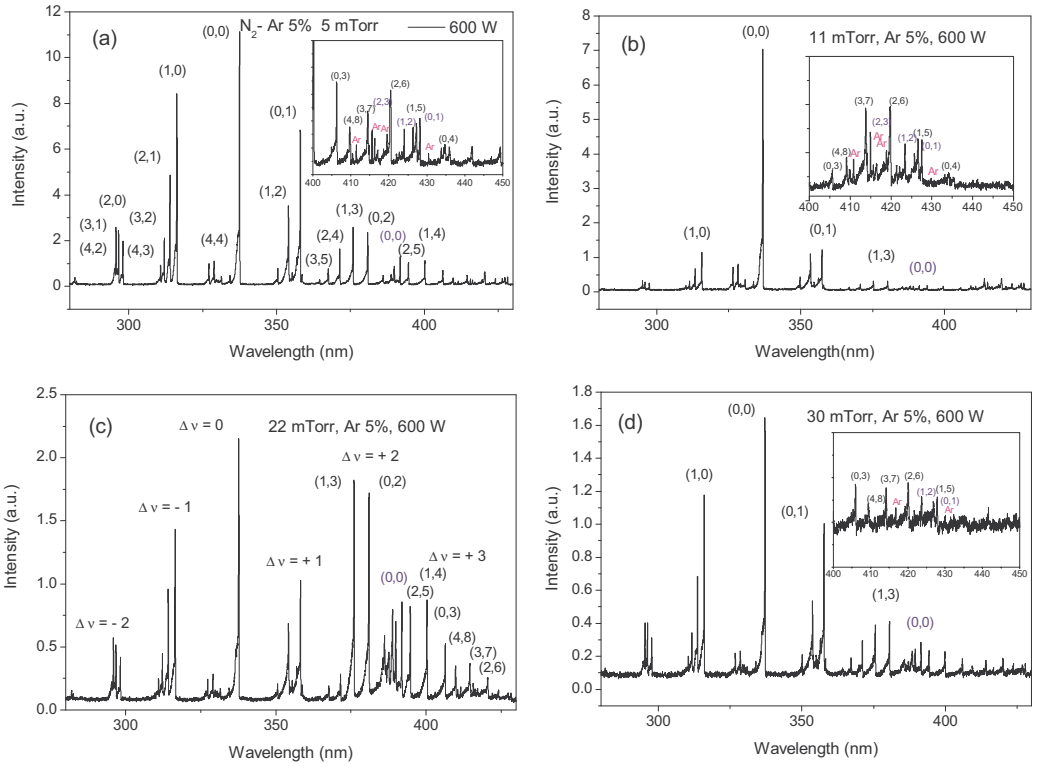

FIG. 4. (Color online) (a) Spectra of optical emission from inductively coupled N_2-5%Ar discharge at $P = 600$ W. The spectra with a range of $250 - 450$ nm at $p = 5$ mTorr, (b) $p = 11$ mTorr, (c) $p = 22$ mTorr, and (d) $p = 30$ mTorr. The insets represent the emission lines between 400 nm and 450 nm.

also deexcitation) increases again at 22 mTorr. In the insets, the spectra in the wavelength range $400 - 450$ nm are shown. The Ar lines ($3p \rightarrow 1s$) at 415.9 nm, 419.8 nm, 430.2 nm, 433.4 nm, and the FNS bands (0,1) at 427.8 nm, (1,2) at 423.6 nm, and (2,3) at 419.9 nm are observed. The Ar $3p \rightarrow 1s$ transition peaks are suppressed as the pressure increases (even though the amount of Ar atoms is increased). This may result from that T_e is decreased with pressure.

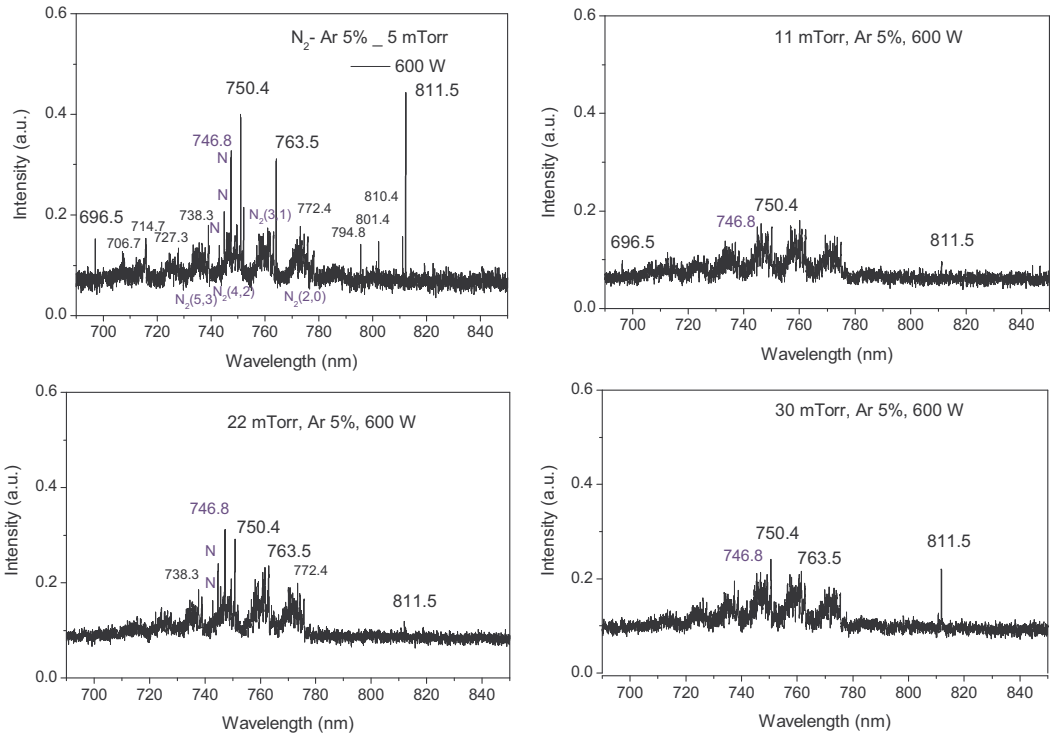

FIG. 5. (Color online) (a) Spectra of optical emission from inductively coupled N_2-5%Ar discharge at $P = 600$ W. The spectra with a range of 690 − 850 nm at $p = 5$ mTorr, (b) $p = 11$ mTorr, (c) $p = 22$ mTorr, and (d) $p = 30$ mTorr.

Figure 5 shows the emission spectra with the wavelength range of 690 − 850 nm from N_2-5%Ar plasmas at several pressures. There exist many Ar peaks at 750.4 nm ($2p_1 \rightarrow 1s_2$), 811.5 nm ($2p_9 \rightarrow 1s_5$), 696.5 nm ($2p_2 \rightarrow 1s_5$), 706.7 nm ($2p_3 \rightarrow 1s_5$), 738.3 nm ($2p_3 \rightarrow 1s_4$), 763.5 nm ($2p_6 \rightarrow 1s_5$), 772.4 nm ($2p_2 \rightarrow 1s_3$), 794.8 nm ($2p_4 \rightarrow 1s_3$), 810.4 nm ($2p_7 \rightarrow 1s_4$), and 801.4 nm ($2p_8 \rightarrow 1s_5$). The N_2 FPS bands (5,3), (4,2), (3,1) and (2,0) are also observed. In addition, the N peaks appear at 746.8 nm ($3p\ ^4S \rightarrow 3s\ ^4P_{5/2}$), 744.2 nm ($3p\ ^4S \rightarrow 3s\ ^4P_{3/2}$), and 742.3 nm ($3p\ ^4S \rightarrow 3s\ ^4P_{1/2}$). As shown in the figure, as the pressure increases, the overall intensities of these lines decrease. The optical spectrum from the 11 mTorr discharge shows a significant change compared to that of the 5 mTorr discharge. The argon peaks except some dominant ones are almost smeared out. This can be explained by that the $2p \rightarrow 1s$ transitions are suppressed since the excitation of the ground state Ar to 2p levels is diminished due to the decrease in T_e with increasing pressure. However, when the gas pressure increased to 22 mTorr, with an abundant supply of nitrogen molecules, the emission from nitrogen atom is clearly seen. At the pressure of 30 mTorr, the N peaks diminish again while the Ar 811.5 nm line becomes high.

Figure 6(a) and 6(b) show the electron density and the electron temperature obtained by a Langmuir probe measurement as a function of the Ar content. With an increase in the Ar content, the electron density increases and the electron temperature decreases. For a fixed power, with an increase of Ar content, the total energy loss per electron-ion pair decreases, hence the electron density increases due to the power balance. This trend is in agreement with the modeling and the experimental works.[16,29,30] Figure 6(c) shows the electron energy probability function (EEPF) for the Ar content of 10 - 30 % at the ICP power of 500 W and the pressure of 1.4 mTorr. In this work, the electron energy probability functions were found to be Maxwellian. The population of electrons with energy greater than 15 eV exhibits an unstable behavior, which might be caused by noise. For nitrogen, the threshold for dissociation is at 9.8 eV; however, the cross section function does not rise significantly until after 15 eV. From there, it rises gradually to a value of $6.74 \times 10^{-17} cm^2$ at 20 eV.[3] Generally, very little N_2 is dissociated because of the high threshold and the peak energy well

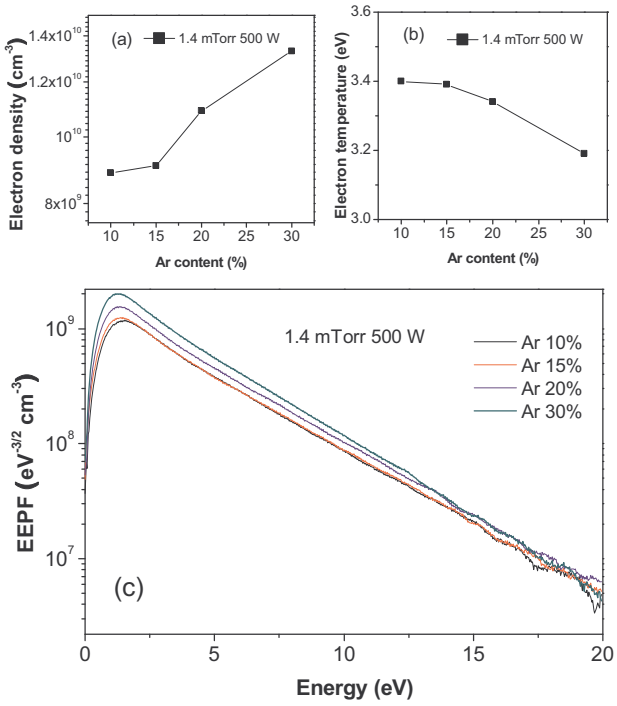

FIG. 6. (Color online) (a) Electron density and (b) electron temperature obtained by using a Langmuir probe. (c) Electron energy probability functions for the Ar contents of 10 - 30 % at $P = 500$ W and p= 1.4 mTorr.

above 20 eV. However, ICP discharges show a considerable amount of high energy electron, and this may promotes the dissociation of N_2. These electrons contribute to an increase in the electron-impact dissociation. In our previous work,[16] it was observed that higher Ar contents resulted in a higher dissociation fraction. This is also related to an increase in the relative production of Ar metastables.

In order to investigate the pressure dependence of n_e, T_e and EEPF, the pressure was varied from 1.4 to 22 mTorr with a fixed power of 500 W. As shown in Fig. 7, the electron density increases first and has a maximum at 11 mTorr, and then slightly decreases with increasing pressure, which is due to the increased collision frequency between electrons and neutral molecules or atoms. The electron temperature decreases with increasing pressure: for the ICP power of 500 W, T_e is about 3.6 eV at 1.4 mTorr, while about 1.7 eV at 22 mTorr. Figure 7(c) shows the measured EEPF with different gas pressures at the ICP power of 500 W. The population of electrons with high energy exhibits an unstable fluctuation. As pressure increases, an easy heating due to a frequent electron-impact rovibrational excitations of nitrogen molecules is thought to contribute to the fluctuation of the probe currents. However, the shape of EEPF roughly remains the Maxwellian distribution. At the pressure of 22 mTorr, there is a significant decrease of the electron energy in the high energy electron region, while the electron density in the low energy electron region does not change much compared to that of 11 mTorr. This can be explained by that the depletion of the high energy electrons around the excitation threshold becomes dominant at the pressure of 22 mTorr.

In order to calculate the dissociation fraction using Eq. (12), the correction factors c_1 and c_2 should be determined. The density of N-metastable, $[N^m(^2D)]$, is about $0.1 - 0.3$ times the density of the ground state species and $[N^m(^2P)]$ is smaller than $[N^m(^2D)]$ by one order of magnitude.[3,31] The excitation rate coefficient $k_{N^m}^{exc}$ is less than k_N^{dir} by a factor of 10 at $T_e = 3$ - 5 eV.[9] Therefore, the excitation from $N^m(^2D)$ to $N^*(3p\ ^4S)$ is small. However, introducing Ar into the nitrogen plasma causes the generation of $N_2(B)$, $N_2(C)$, $N_2^+(X)$ and $N_2^+(B)$.[32] The interaction of these with the ground state nitrogen atoms may result in the enhancement of $[N^m]$. But, the change of $[N^m]$ with the Ar

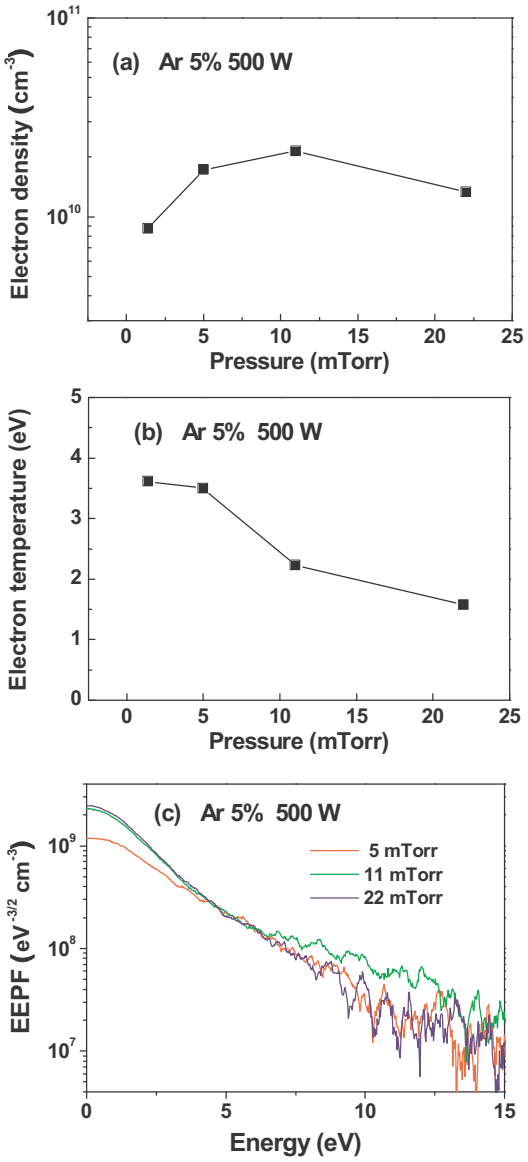

FIG. 7. (Color online) (a) Electron density, (b) electron temperature, and (c) electron energy probability functions as a function of pressure at the Ar content of 5 % and $P = 500$ W.

content will not be considered in the analysis of this study. Dissociative excitation rate coefficient $k_{N_2}^{diss-exc}$ is less than k_N^{dir} by a factor of 1000 at $T_e = 3$ - 5 eV.[9] Then the factor c_1 is written as

$$c_1 \approx 0.1\frac{[\mathrm{N^m}]}{[\mathrm{N}]} + 0.001\frac{[\mathrm{N_2}]}{[\mathrm{N}]} + \frac{[\mathrm{Ar^m}][\mathrm{N}]k_N^{Penn} + [\mathrm{Ar^m}][\mathrm{N_2}]k_N^{Penn-diss}}{n_e[\mathrm{N}]k_N^{dir}}. \quad (13)$$

In fact, the term $[\mathrm{Ar^m}][\mathrm{N_2}]k_N^{Penn-diss}$ represents the Penning dissociation followed by the Penning excitation due to Ar excited states.[33] The rate coefficient for this reaction is hardly found in the literature. The rate coefficients $k_N^{Penn} = 3 \times 10^{-11}$ cm^3/s and two values of $k_N^{Penn-diss} = 3 \times 10^{-11}$ or 3×10^{-12} cm^3/s are used. Utilizing equation (9) with the measured n_e and T_e, $[\mathrm{Ar^m}]$ can be obtained. At $p = 1.4$ mTorr, the values of $[\mathrm{Ar^m}]/[\mathrm{Ar}]$ were found as: 0.0178 % (Ar 10 %), 0.0216 % (Ar 15 %), 0.0237 % (Ar 20 %), 0.0235 % (Ar 30 %). Utilizing the obtained values of $[\mathrm{N}]/[\mathrm{N_2}]$ (without correction) and assuming $[\mathrm{N^m}]/[\mathrm{N}] \approx 0.1$, we can estimate the correction factors: c_1 are

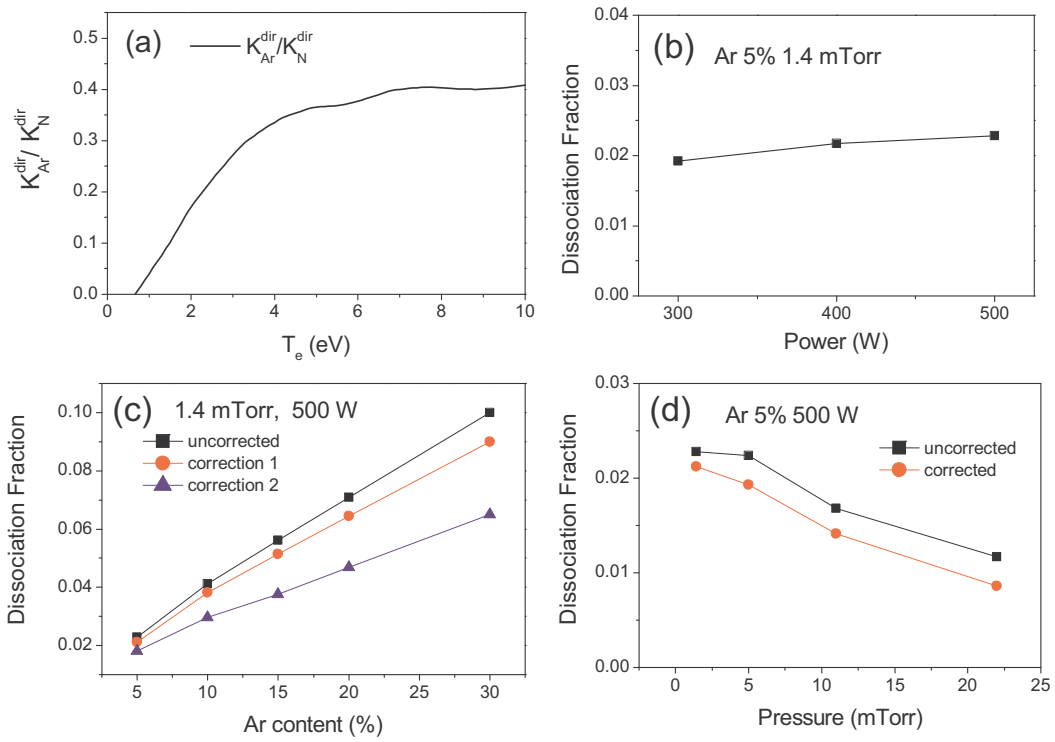

FIG. 8. (Color online) (a) Ratio of the rate coefficients k_{Ar}^{dir}/k_N^{dir}, (b) Dissociation fraction as a function of power at $p =$ 1.4 mTorr and the Ar content 5%, (c) Dissociation fraction versus the Ar content at $p = 1.4$ mTorr and $P = 500$ W, where the uncorrected and two kind of corrected estimations are presented (correction 1: $k_N^{Penn-diss} = 3 \times 10^{-12}$ cm^3/s, correction 2: $k_N^{Penn-diss} = 3 \times 10^{-11}$ cm^3/s). (d) Dissociation fraction as a function of pressure at $P = 500$ W and the Ar content 5%. Uncorrected and correction 1 results are plotted.

0.0793 - 0.266 (Ar 5 %), 0.0823 - 0.388 (Ar 10 %), 0.0971 - 0.497 (Ar 15 %), 0.103 -0.519 (Ar 20 %), 0.115 - 0.542 (Ar 30 %) (the lower bound corresponds to the case of $k_N^{Penn-diss} = 3 \times 10^{-12}$ cm^3/s, the upper bound $k_N^{Penn-diss} = 3 \times 10^{-11}$ cm^3/s) and c_2 are 0.00183 (Ar 5 %), 0.00213 (Ar 10 %), 0.00262 (Ar 15 %), 0.00289 (Ar 20 %), and 0.00307 (Ar 30 %). In this calculation, the neutral particle densities are obtained using the relation $[N_2] = p\, x_{N_2}/k_B T_{rot}$.[16]

Figure 8(a) represents the ratio of rate coefficients k_{Ar}^{dir}/k_N^{dir} used in this work. The values of the electron impact excitation cross sections are obtained from the literature.[34,35] In deriving the rate coefficient, a Max-well-Boltzmann energy distribution of electrons was assumed. The determination of dissociation fraction via actinometry is convenient because the necessary parameters are the electron temperature and the emission intensity ratio of nitrogen atom peak and argon peak. However, the actinometric method has some drawback in providing accurate results because of the larger errors on the excitation cross section data[34–38] and of the assumption of Maxwell-Boltzmann energy distribution of electrons. All these factors contribute to a limited accuracy of the actinometric method.

Figure 8(b) shows the estimated dissociation fraction of N_2 as functions of power at the pressure 1.4 mTorr for the Ar content of 5%. The dissociation fraction increased with increasing power from 1.92 % at 300 W to 2.28 % at 500 W. The dissociation fraction versus the Ar content is shown in figure 8(c), where the uncorrected and two kind of corrected estimations are presented. As was shown in the previous works, the dissociation fraction increases with the Ar content. As expected, the correction factor reduces the value of dissociation fraction and becomes more important at higher Ar contents. If one utilizes the larger value of $k_N^{Penn-diss}$ (that is, the Penning dissociation followed by the Penning excitation due to Ar excited states is fully considered), one can obtain a lower dissociation fraction (designated as correction 2 in Fig. 8(c)). The pressure dependence

of the dissociation fraction is represented in figure 8(d). The dissociation fraction decreased with increasing pressure. The values of dissociation fraction were well comparable to those obtained by vacuum ultraviolet emission spectroscopy performed by Nakano *et al.*[13] and to the result of global modeling.[31] The pressure dependence of the dissociation fraction was similar to the results of earlier works.[6,31] The observed decrease in dissociation fraction with pressure is expected to be due to increased wall recombination and also potentially due to the decreased electron-neutral collisional frequency at higher pressures.[3]

To explore the dependence of dissociation fraction on plasma parameters, a simple scaling relation can be utilized. Neutral nitrogen atoms are assumed to be generated mainly by electron-impact dissociation of N_2 (and partly by the Penning dissociation due to the excited Ar), and to be lost by diffusion to and recombination at the reactor wall and by the electron-impact ionization of N. There is also another contribution to N-atom production: charge exchange between nitrogen molecules and argon ions followed by dissociative recombination.[9] But this can be neglected in nitrogen-rich plasmas. In addition, the creation of nitrogen atoms resulting from the dissociation of vibrationally excited $N_2(X, v)$ molecules past a threshold vibrational level ($v = 45$) and the loss due to the volume recombination occurring through a three-body collision process involving molecular nitrogen should be also considered.[14,15] These addition terms are especially important for higher pressure plasmas such as microwave-sustained discharges. Then we have

$$2K_{diss}n_e[\mathrm{N_2}] + 2K_{V-V}[\mathrm{N_2}][\mathrm{N_2}(X, v = 45)] + k_N^{Penn-diss}[\mathrm{Ar^*}][\mathrm{N_2}] \approx (K_d + k_{iz}^N n_e)[\mathrm{N}] + 2K_{rec}[\mathrm{N}][\mathrm{N}][\mathrm{N_2}], \tag{14}$$

where K_{diss} is the rate coefficient for electron-impact dissociation of N_2, K_{V-V} for dissociation from vibrationally excited $N_2(X, v)$ molecules, k_{iz}^N for the electron-impact ionization of N, K_d for the diffusion to and recombination at the reactor wall of N atoms, and K_{rec} for recombination through a three-body collision process. Assuming that metastable Ar plays an important role, the dissociation fraction is approximated by

$$\frac{[\mathrm{N}]}{[\mathrm{N_2}]} \approx \frac{2K_{diss}n_e + 2K_{V-V}[\mathrm{N_2}(X, v = 45)] + k_N^{Penn-diss}[\mathrm{Ar^m}]}{K_d + k_{iz}^N n_e + 2K_{rec}[\mathrm{N}][\mathrm{N_2}]} \tag{15}$$

If K_{diss} and k_{iz}^N are assumed to have Arrhenius forms $K_{diss} = K_{diss0}e^{-\varepsilon_{diss}/T_e}$, $k_{iz}^N = k_{iz0}e^{-\varepsilon_{iz}/T_e}$ (ε_{diss} (= 9.8 eV) and ε_{iz} (= 14.5 eV) are the threshold energies for dissociation and ionization reactions),[39] then K_{diss} and k_{iz}^N decrease with decreasing electron temperature (k_{iz}^N has a steeper variation). It is worth noting that if we look into the electron energy dependence of the cross section of nitrogen dissociation, ε_{diss} should be replaced by the real activation energy which is a little higher than the threshold energy (but lower than ε_{iz}).

It is observed that as pressure is increased, n_e increases first and then slightly decreases, while T_e decreases. The electron impact reaction rates show an exponential dependence on T_e and generally exhibits linear variations in n_e. The $k_{iz}^N n_e$ decreases dominantly over $K_{diss}n_e$ with a decrease in T_e (indicated as $\Downarrow$ below). An increase in pressure decreases the diffusion to and recombination at the walls.[3] The contribution from vibrational excitation of $N_2(X, v)$ followed by dissociation to N atoms is enhanced with increasing pressure due to an increase in the vibrational temperature. Therefore, with an increase of the pressure at a fixed Ar percentage, we have a simple scaling:

$$p \uparrow, [\mathrm{Ar}] \uparrow, [\mathrm{N_2}] \uparrow, n_e \uparrow, T_e \downarrow, K_d \downarrow, k_{iz}^N \Downarrow, K_{diss} \downarrow, [\mathrm{Ar^m}] \uparrow, K_{V-V} \uparrow, [\mathrm{N}]/[\mathrm{N_2}] \downarrow . \tag{16}$$

The dissociation fraction was observed to decrease slightly with pressure. The nitrogen atom densities increase with pressure because the initial density of molecular species is increased with pressure. In the pressure range of 1.4 - 30 mTorr, the dissociation fraction decreased. The observed decrease in dissociation fraction with pressure is mainly due to a decrease in T_e in addition to the increased wall recombination and due to the decreased electron-neutral collision frequency. As the power is increased, the dissociation fraction is observed to increase. From the global balance of the discharge

kinetics, the dissociated neutral atom density is expected to be proportional to the power.[31,39] The trend of change in the dissociation fraction correlates well with the n_e, T_e, and the EEPF.

IV. CONCLUSION

A detailed diagnostic study of low-pressure inductively coupled N_2-Ar plasmas by using OES and Langmuir probe was performed under the conditions of nitrogen pressures in the range of 1.4 - 30 mTorr and ICP powers of 300 - 600 W. The effect of gas pressure on the characteristics of optical emission from discharges was investigated. The complicated variations in the emission intensities of atomic lines and molecular bands resulted from the changes of n_e, T_e, and neutral particle densities with pressure. The electron density was found to increase and the electron temperature decreased with increasing Ar content. With increasing pressure, the electron density increased first and had a maximum at 11 mTorr, and then slightly decreased. As expected, the electron temperature decreased with pressure. The EEPFs were roughly Maxwellian over the operating parameter range of this study. The correction factors for the dissociation fraction of nitrogen molecules accounting for Ar effect was formulated and calculated. The correction factors became important as the Ar content increased. The dissociation fraction measured by using OES actinometry increased with increasing Ar content and power as expected. For the pressure range of 1.4 - 30 mTorr in the Ar 5% -N_2 discharge, the dissociation fraction decreased with pressure and had values ranging 0.86 - 2.12%. The formulated correction factor can be utilized to provide a reasonable value of dissociation fraction for various N_2-Ar plasmas in broad operating conditions.

ACKNOWLEGMENT

This research was supported by Basic Science Research Program through the National Research Foundation of Korea(NRF) funded by the Ministry of Education, Science and Technology (grant number 2009-0070839)

[1] M. Abdel-Rahman, V. Schulz-von der Gathen, T. Gans, K. Niemi, and H. F. Dobele, Plasma Sources Sci. Technol. **15**, 620 (2006).
[2] N. Itagaki, S. Iwata, K. Muta, A. Yonesu, S. Kawakami, N. Ishii, Y. Kawai, Thin Solid Films **435**, 259 (2003).
[3] M. A. Worsley, S. F. Bent, N. C. M. Fuller, and T. Dalton, J. Appl. Phys. **100**, 083301 (2006).
[4] M. Tabbal, M. Kazopoulo, T. Christidis, and S. Isber, Appl. Phys. Lett. **78**, 2131 (2001).
[5] R. W. McCullough, J. Geddes, J. A. Croucher, J. M. Woolsey, D. P. Higgins, M. Schlapp, and H. B. Gilbody, J. Vac. Sci. Technol. A **14**, 152 (1996).
[6] D. Voulot, R. W. McCullough, W. R. Thompson, D. Burns, J. Geddes, Q. J. Gosimini, E. Nelson, P. P. Chow, and J. Klaassen, J. Vac. Sci. Technol. A **16**, 3434 (1998).
[7] T. Kimura and H. Kasugai, J. Appl. Phys. **108**, 033305 (2010).
[8] S. Tada, S. Takashima, M. Ito, M. Hori, T. Goto, and Y. Sakamoto, J. Appl. Phys. **88**, 1756 (2000).
[9] T. Czerwiec, F. Greer, and D. B. Graves, J. Phys. D:Appl. Phys. **38**, 4278 (2005).
[10] D. Douai, J. Berndt, and J. Winter, Plasma Sources Sci. Technol. **11**, 60 (2002).
[11] V. Henriques, E. Tatarova, F. M. Dias, and C. M. Ferreira, J. Appl. Phys. **91**, 5632 (2002).
[12] Y. Wang, R. J. Van Brunt, and J. K. Olthoff, J. Appl. Phys. **83**, 703 (1998).
[13] T. Nakano, S. Kumagai, and S. Samukawa J. Appl. Phys. **92**, 2990 (2002).
[14] P. A. Sa and J. Loureiro, J. Phys. D: Appl. Phys. **30**, 2320 (1997).
[15] P. Merel, M. Tabbal, M. Chaker, M. Moisan and A. Ricard, Plasma Sources Sci. Technol. **7**, 550 (1998).
[16] M. A. Song, Y. W. Lee, and T. H. Chung, Phys. Plasmas **18**, 023504 (2011).
[17] M. V. Malyshev and V. M. Donnelly, J. Appl. Phys. **87**, 1642 (2000).
[18] D. C. Seo, T. H. Chung, and H. J. Yoon, J. Appl. Phys. **89**, 4219 (2001).
[19] K. Okada, S. Komatsu, and S. Matsumoto, J. Vac. Sci. Technol. A **17**, 721 (1999).
[20] J. Hong, A. Granier, C. Leteinturier, M. Peignon, and G. Turban, J. Vac. Sci. Technol. A **18** 497 (2000).
[21] C. Foissac, C. Dupret and P. Supiot, J. Phys. D: Appl. Phys. **42**, 015206 (2009).
[22] H. A. Hyman, Phys. Rev. A **18**, 441 (1978).
[23] H. A. Hyman, Phys. Rev. A **20**, 855 (1979).
[24] V. M. Donnelly, J. Phys. D: Appl. Phys. **37**, R217 (2004).
[25] A. Dasgupta, M, Blaha, and J. L. Giuliani, Phys. Rev. A **61**, 012703 (1999).
[26] J. E. Velazco, J. H. Kolts, and D. W. Setser, J. Chem. Phys. **69**, 4357 (1978).
[27] S. Agarwal, B. Hoex, M. C. M van de Sanden, d. Maroudas, E. S. Aydil, Appl. Phys. Lett. **83**, 4918 (2003).
[28] N. K. Bibinov, A. A. Fateev, and K. Wiesemann, J. Phys. D: Appl. Phys. **34**, 1819 (2001).
[29] J. Ma and Y. K. Pu, Phys. Plasmas **10**, 4118 (2003).

[30] Y. M. Shin, E. Y. Kim, and T. H. Chung, J. Korean Phys. Soc. **53**, 617 (2008).
[31] E. G. Thorsteinsson and J. T. Gudmundsson, Plasma Sources Sci. Technol. **18**, 045001 (2009).
[32] V. Linss, H. Kupfer, S. Peter, and F. Richter, J. Phys. D: Appl. Phys. **37**, 1935 (2004).
[33] A. Davison, J. C. Avelar-Batista, A. D. Wilson, A. Leyland, A. Matthews, and K. S. Fancey, J. Vac. Sci. Technol. A **21**, 1683 (2003).
[34] R. M. Frost, P. Awakowicz, H. P. Summers, and N. R. Badnell, J. Appl. Phys. **84**, 2989 (1998).
[35] J. K. Ballou, C. C. Lin and F. E. Fajen, Phys. Rev. A **8**, 1797 (1973).
[36] J. B. Boffard, G. A. Piech, M. F. Gehrke, M A Lagus, L. W. Anderson and C. C. Lin, J. Phys. B **29**, L795 (1996).
[37] J. B. Boffard, G. A. Piech, M. F. Gehrke, L. W. Anderson and C. C. Lin, Phys. Rev. A **59**, 2749 (1999).
[38] V. Puech, and L. J. Tonhin, Phys. D: Appl. Phys. **19**, 2309 (1986).
[39] M. A. Lieberman and A. J. Lichtenberg, *Principles of Plasma Discharge and Materials Processing* (Wiley, New York, 1994), p.487.